Chinese Chemical Letters 37 (2026) 110064

Contents lists available at ScienceDirect

Chinese Chemical Letters

journal homepage: www.elsevier.com/locate/cclet

Optimizing COF crystallinity for high-resolution GC separation

Chu Zeng, Han Yang, Ming Xu*, Zhi-Yuan Gu*

Jiangsu Key Laboratory of Biofunctional Materials, Jiangsu Collaborative Innovation Center of Biomedical Functional Materials, Jiangsu Key Laboratory of New Power Batteries, College of Chemistry and Materials Science, Nanjing Normal University, Nanjing 210023, China

ARTICLE INFO

Article history:
Received 21 March 2024
Revised 18 April 2024
Accepted 27 May 2024
Available online 3 June 2024

Keywords:
Covalent organic framework
Gas chromatography
Crystallinity
Kinetic diffusion
Thermodynamic adsorption

ABSTRACT

This research explores the influence of crystallinity on gas chromatographic (GC) separation using covalent organic frameworks (COFs) as stationary phases. Three COF materials (CTF-DCBs) with varying crystallinity were synthesized and characterized. CTF-DCB-1, with superior crystallinity, demonstrated high-selectivity GC separation of benzene isomers as well as styrene/phenylacetylene mixtures, while CTF-DCB-2 and CTF-DCB-3 exhibited lower crystallinity and worse separation performance. Thermodynamic and kinetic tests showed that CTF-DCB-1 had the worst thermodynamic adsorption but low diffusion mass transfer resistance, which resulted in the best separation. Therefore, optimizing the crystallinity of COFs is necessary for balancing the kinetic diffusion and thermodynamic interactions towards the analytes, achieving high-performance GC stationary phases.

© 2025 Published by Elsevier B.V. on behalf of Chinese Chemical Society and Institute of Materia Medica, Chinese Academy of Medical Sciences.

Separation medium is the essence of separation science. Developing effective stationary phases is crucial for advancing the capabilities of gas chromatography (GC) and achieving optimal performance in analytical separations. Recently, crystal porous materials, such as metal-organic frameworks (MOFs) [1-5] and covalent organic frameworks (COFs) [6-10], have been reported as high-performance GC stationary phases due to their specific properties which can balance the thermodynamic interactions towards analytes and the kinetic diffusion of analytes. Some of these stationary phases exhibit exceedingly higher separation ability than the commercial ones [5,11].

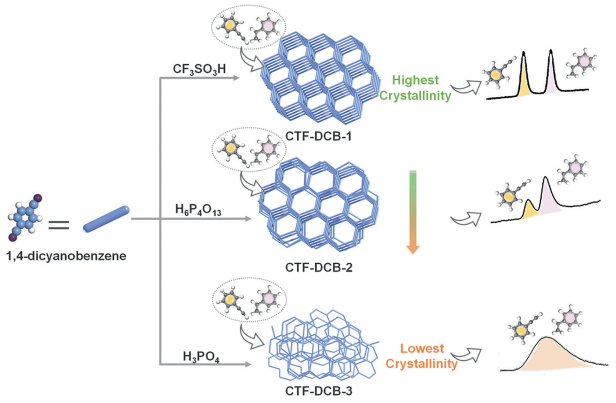
Crystal porous materials suffer from the problem of different crystallinity according to different synthesis methods. For example, although UiO-66 [12] can be synthesized by adding diverse monotopic acids as modulators [13,14], its crystallinity is directly affected by the amount and type of the modulators [15]. Solvent effects, monomer geometry structure, and type of catalyst all affect the crystallinity of COF [16-18]. Theoretically, the crystallinity of porous materials leads to different exposed active sites and pore size distributions, which influence the application performance of their original structures. Taking the low crystallinity of these materials as an example, on the one hand, the low crystallinity brings in more exposed bonding sites for the combination of analytes, resulting in stronger thermodynamic interactions and faster association rates. Researchers usually create defects in ideal MOFs to enhance their adsorption capacity [19,20] and catalytic activity [21,22]. On the other hand, the low crystallinity interferes with the pore size distribution of the original porous materials, leading to disordered diffusion paths. Reports indicated that disordered diffusion paths exhibited substantial barriers to the diffusion of analytes [23,24]. Thus, the crystallinity of the porous materials can affect the equilibrium point of the kinetic diffusion and thermodynamic interactions towards the analytes. Given the prevalence of varying crystallinity in porous materials, exploring the connection between crystallinity and their separation capabilities is crucial in the design of high-performance GC stationary phases.

The porous material COFs consist of regularly arranged organic building blocks linked together by robust covalent bonds [25]. With elevated thermal and chemical stability, significant porosity, and diverse interaction sites, COFs prove highly suitable for deployment as GC stationary phases [7]. Notably, the crystalline properties of COFs can be effectively modulated through changing the synthetic approaches [26-28]. Thus, COFs were selected for this study to explore the correlation between crystallinity and their efficacy in separation.

Here, a covalent triazine framework (CTF) incorporating 1,4-dicyanobenzene (DCB) [29,30] as the building block was selected as the focus material for investigation (Scheme 1). The crystalline properties of the derived CTF-DCB were meticulously controlled by employing various modulators. Specifically, the introduction of CF_3SO_3H, $H_6P_4O_{13}$, and H_3PO_4 led to the formation of CTF-DCB-1 with the highest crystallinity, CTF-DCB-2 with moderate crystallinity, and CTF-DCB-3 with the lowest crystallinity, respectively. The three materials were coated on the inner wall of the capil-

* Corresponding authors.
E-mail addresses: mingxu@njnu.edu.cn (M. Xu), guzhiyuan@njnu.edu.cn (Z.-Y. Gu).

https://doi.org/10.1016/j.cclet.2024.110064
1001-8417/© 2025 Published by Elsevier B.V. on behalf of Chinese Chemical Society and Institute of Materia Medica, Chinese Academy of Medical Sciences.



Scheme 1. The schematic diagram of investigating the connection between crystallinity and their separation capabilities using CTF-DCB with different crystallinities.

lary for the separation of different analytes. Analysis of the thermodynamic adsorption enthalpy (ΔH) and adsorption entropy (ΔS) through the van't Hoff equation revealed that CTF-DCB-3 exhibited the highest adsorption towards analytes, resulting in greater difficulty in desorption. Conversely, CTF-DCB-1 displayed the weakest thermodynamic adsorption, leading to the fast adsorption and desorption. Besides, the kinetic diffusion coefficient of analytes in the stationary phase (D_s) calculated based on the Golay equation [31,32] showed that CTF-DCB-1 presented the least restrictive diffusion barrier, whereas CTF-DCB-2 exhibited a notably larger diffusion barrier. The separation results proved that the CTF-DCB-1, which exhibited the best crystallinity, performed the best separation ability, while CTF-DCB-2 and CTF-DCB-3 exhibited progressively worse performance. Thus, only with high crystallinity, the CTF-DCB can effectively reconcile thermodynamic interactions with analytes and kinetic diffusion of analytes, resulting in high separation performance.

The CTF-DCB crystals with different crystallinities were synthesized according to the previous reports without any changes. The CTF-DCB-1 [29] underwent polymerization of DCB catalyzed by CF_3SO_3H under microwave conditions for 20 min. The CTF-DCB-2 and CTF-DCB-3 [30] were prepared by the nitrile trimerization of DCB catalyzed by $H_6P_4O_{13}$ and H_3PO_4, respectively, in Pyrex tubes at a temperature of 400 °C (Fig. S1 in Supporting information). Detailed procedural steps can be found in Supporting information.

The CTF-DCBs possessed a typical AA-stacking structure with a one-dimensional channel of about 1.1 nm (Figs. 1a and b). The powder X-ray diffraction (PXRD) patterns of all the synthesized CTF-DCBs exhibited identical diffraction peaks that closely corresponded to the simulated ones (Fig. 1c), proving the successful synthesis. The peaks at 7°, 12°, 14°, and 27° represented the (100), (110), (200), and (001) planes, respectively. The diffraction peaks of CTF-DCB-1 exhibited the sharpest profile and the least peak broadening among the three materials, indicating its highest level of crystallinity. In contrast, the diffraction peaks of CTF-DCB-3 displayed significant broadening with a low signal-to-noise ratio, confirming the lowest crystallinity. However, the peaks of CTF-DCB-2 were not as sharp as those of CTF-DCB-1, and the peak broadening was not substantial, indicating a moderate level of crystallinity.

The thermal stability of the three CTF-DCBs was assessed through thermogravimetric analysis (TGA). As depicted in Fig. 1d, the CTF-DCBs exhibited a minor decrease in mass (<10 %) before reaching a temperature of 618 °C. This phenomenon could be attributed to the evaporation of water molecules or detergents and catalysts adsorbed by the frameworks during the preparation process at higher temperatures. The negligible mass loss at this stage also indicated the favorable thermal stability of all the CTF-

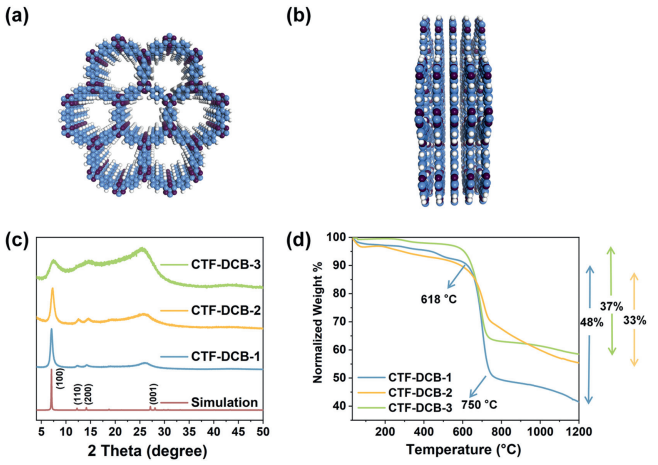


Fig. 1. The schematic structure of CTF-DCBs observed from the *c*- (a) and *a*- (b) axes. (c) The PXRD patterns of the synthesized and simulated CTF-DCBs. (d) The TGA curves of the synthesized CTF-DCBs.

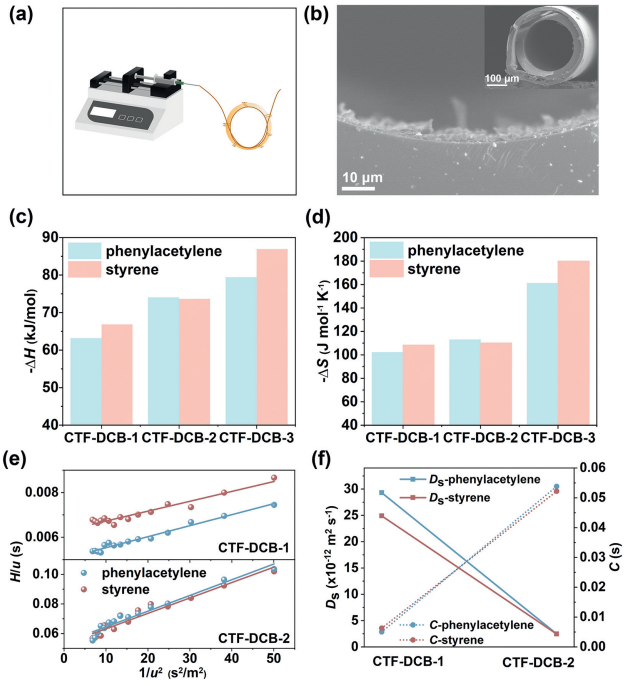


Fig. 2. (a) The diagram of the dynamic coating method. (b) The SEM images of the CTF-DCB-1 coated column. (c) The ΔH and (d) the ΔS of styrene and phenylacetylene in the CTF-DCBs coated columns. (e) Diffusion coefficient diagram for styrene and phenylacetylene in CTF-DCB-1 and CTF-DCB-2 coated columns. (f) The D_s and *C* of styrene and phenylacetylene in CTF-DCB-1 and CTF-DCB-2 coated columns.

DCBs. Beyond 618 °C, the CTF-DCBs underwent substantial mass loss due to collapse and structural decomposition. Notably, among the frameworks, CTF-DCB-1 showed the greatest mass loss at 48 %, suggesting a higher concentration of ligands in its structure. This observation further supported its highest level of crystallinity.

After synthesis and characterization, the CTF-DCBs were individually coated onto capillary columns using a straightforward dynamic coating method (Fig. 2a) [33,34]. 3-Aminopropyl triethoxysilane (APTES) used before coating is a binder that modifies columns by providing amino groups. Without APTES, the column separation performance deteriorates (Fig. S2 in Supporting information). In summary, a 2 mL ethanol suspension (2 mg/mL) of the prepared CTF-DCBs was introduced into a capillary column. Subsequently, the column underwent flushing with N_2 at a velocity of

30 cm/min to eliminate excess ethanol suspension. The resulting capillary columns were then conditioned at 250 °C for 240 min. The cross-section of CTF-DCB-1 coated capillary column segments was visible in the SEM images. As Fig. 2b and Fig. S3 (Supporting information) indicated, the material coating on the inner wall was evenly distributed with a thickness of approximately 0.5 μm.

To compare the thermodynamic interactions among CTF-DCBs with different crystallinities and analytes, phenylacetylene and styrene were employed as illustrative examples. These analytes were specifically chosen due to the significance of styrene as a crucial chemical intermediate and the common occurrence of phenylacetylene as an impurity during styrene production. The temperatures at different analytes peak in various columns vary greatly, and choosing the same temperature can result in some peaks being inseparable from air peaks. Therefore, appropriate temperatures were chosen for different columns to carry out the determination of the enthalpy of adsorption. The ΔH and ΔS of these compounds onto different columns were determined through the application of the van't Hoff equation:

$$\ln k' = -\frac{\Delta H}{RT} + \frac{\Delta S}{R} + \ln\varphi$$

where R is the universal gas constant ($R = 8.314\ \mathrm{J\ mol^{-1}\ K^{-1}}$), T is the detection temperature (K), and φ is the volume ratio of the solid stationary phase to the mobile stationary phase ($\varphi = 7.984 \times 10^{-3}$).

The van't Hoff plots for each analyte on the three columns revealed strong linear correlations, underscoring the consistent interaction between the analytes and the pores of the covalent organic framework throughout the separation process (Fig. S4 in Supporting information). From CTF-DCB-1 to CTF-DCB-2 and CTF-DCB-3, the ΔH values for both analytes exhibited a gradual shift towards negativity (Fig. 2c, Table S1 in Supporting information). This observation suggested that as crystallinity decreases, CTF-DCBs demonstrate increasing interactions with analytes. We supposed that this trend was attributable to the heightened presence of defects introduced by lower crystallinity, serving as accessible adsorption sites for the analytes. Moreover, CTF-DCB-1 and CTF-DCB-3 displayed the capability to discern variations in adsorption interactions towards phenylacetylene and styrene, whereas CTF-DCB-2 did not. Parallel to the trend in ΔH, the ΔS values of the analytes became more negative from CTF-DCB-1 to CTF-DCB-2 and CTF-DCB-3 (Fig. 2d). Notably, the ΔS values for analytes on the CTF-DCB-3 coated column surpassed those on the other two columns. This phenomenon implied that analytes experienced the least conformational freedom and were most constrained within the pores of CTF-DCB-3, indicating strong interactions. The ΔS values further proved that the strength of thermodynamic interactions between CTF-DCBs and the analytes was inversely proportional to the crystallinity.

To compare the kinetic diffusion of analytes influenced by crystallinity, diffusion tests were performed at 190 °C with styrene and phenylacetylene as target analytes by GC. The CTF-DCB-3 coated column was not discussed here due to rather poor diffusion. The kinetic diffusion constants and the mass transfer coefficients have been calculated from the Golay equation [31,32] follows (Fig. 2e):

$$H = \frac{B}{u} + C \times u$$

$$C = \frac{1 + 6k' + 11k'^2}{24\left(1 + k'\right)^2} \times \frac{r^2}{D_g} + \frac{2}{3} \times \frac{k'}{\left(1 + k'\right)^2} \times \frac{d_f^2}{D_s}$$

where H is the height equivalent to a theoretical plate, B/u is the longitudinal diffusion, $C \times u$ is the mass transfer term, D_s is the diffusion coefficient of the analytes in the stationary phase, D_g is the diffusion coefficient of the analytes in the mobile phase, k' is the retention factor, r is the internal radius of the capillary column without the coating layer and d_f is the thickness of the coating layer.

The obviously different C values indicated a more pronounced diffusion barrier for both styrene and phenylacetylene within the CTF-DCB-2 and CTF-DCB-1 coated columns (Fig. S5 and Table S2 in Supporting information). Meanwhile, the D_s values of the analytes were considerably greater in the CTF-DCB-1 than in the CTF-DCB-2 (Fig. 2f), demonstrating a faster diffusion of analytes in CTF-DCB-1 compared to CTF-DCB-2. This discrepancy arises from the superior crystallinity of CTF-DCB-1, featuring a more uniform pore size distribution that facilitates the creation of well-ordered diffusion paths. Conversely, the lower crystallinity of CTF-DCB-2 introduces defects into the material, resulting in relatively disordered diffusion paths. As such, we inferred that the mass transfer rate of analytes was directly proportional to the crystallinity of CTF-DCBs.

The separation abilities of CTFs were then evaluated using different gas mixtures as analytes. Before initiating the GC separation, baseline tests were collected on three columns. The smooth profiles of all three baselines indicated the absence of contaminants in the CTF-DCB-coated capillary columns (Fig. S6 in Supporting information). Styrene and phenylacetylene mixture were first used as the separation target. The separation conditions are exhibited in Table S3 (Supporting information). As shown in Figs. 3a-d, it was evident that the CTF-DCB-1 column successfully achieved baseline separation for this group of unsaturated analogs. The separation resolution of styrene and phenylacetylene was 2.68 (Table S4 in Supporting information). The elution sequence of styrene and phenylacetylene was in accordance with their boiling point. However, the separation performance of the CTF-DCB-2 coated column was less satisfactory (Figs. 3e and f). The over-strong thermodynamic interactions and high diffusion barrier provided by CTF-DCB-2 deflected the optimized separation equilibrium point, resulting in this significantly lower separation resolution compared to CTF-DCB-1. The CTF-DCB-3 showed even worse separation ability because of the highest thermodynamic interactions and the lowest mass transfer (Figs. 3g and h). When separating other analytes such as xylene, dibromobenzene, trichlorobenzene, and dichlorobenzene isomers, CTF-DCB-1 still showed the highest separation ability, followed by CTF-DCB-2 and CTF-DCB-3 (Figs. S7-S9 in Supporting information). The phenomena further proved that the highest crystallinity of CTF-DCB-1 achieved the equilibrium of the kinetic diffusion and thermodynamic interactions, leading to this good separation ability. In addition, the pore sizes of the better crystallized CTF-DCB-1 and CTF-DCB-2 are obviously smaller than those of the amorphous CTF-DCB-3 [29,30]. Thus, the faster diffusion of analytes in CTF-DCB-3 resulted a shorter time to peak despite its high adsorption enthalpy. Moreover, after storage for 2 years within a temperature range of 273–300 K and a humidity range of 50 %–70 %, the CTF-DCB-1 coated column was utilized to re-separate xylene isomers. The separation results demonstrated that the separation resolution of CTF-DCB-1 columns remained consistent after an extended storage period, indicating remarkable stability and reproducibility of this CTF-DCB-1 coated column (Fig. 3b).

In conclusion, the relationships between the COFs' crystallinity, the thermodynamic interactions, and the diffusion kinetic of analytes were evaluated. Our results proved that the strength of thermodynamic interactions between CTF-DCBs and the analytes was inversely proportional to the crystallinity, while the diffusion kinetic of analytes was directly proportional to the crystallinity of CTF-DCBs. Although CTF-DCB-3 with low crystallinity may showcase enhanced thermodynamic interactions, its disordered pores significantly impeded GC separation efficiency. In contrast, the well-ordered pore channels of CTF-DCB-1 enabled the

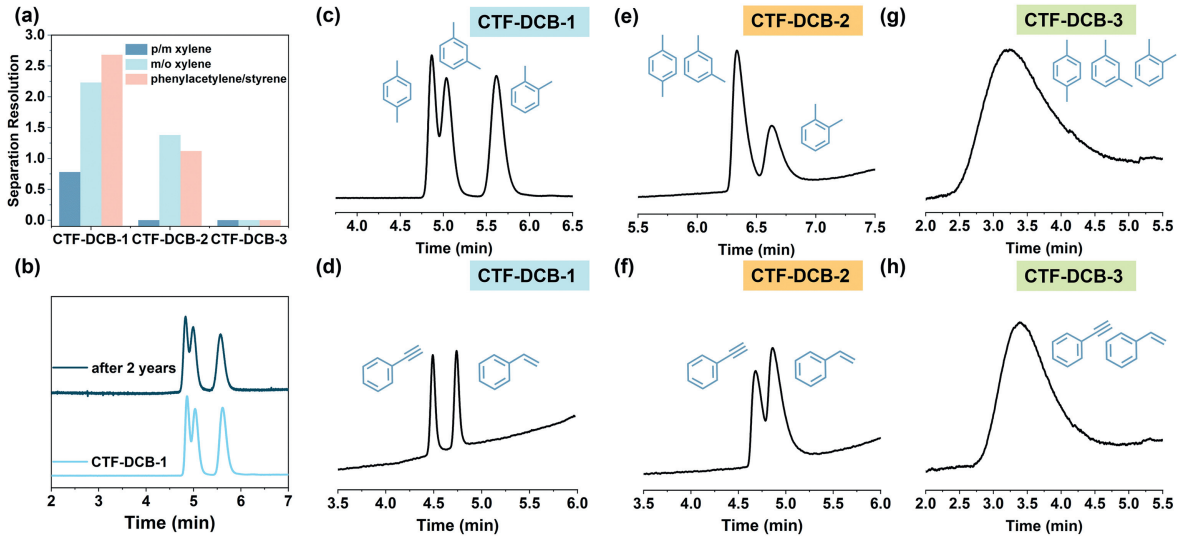


Fig. 3. (a) The separation resolution (R_s) of different analytes in three CTF-DCBs coated columns. (b) The chromatograms of xylene isomers in CTF-DCB-1 coated column after the storage of 2 years. The chromatograms of xylene isomers in (c) CTF-DCB-1, (e) CTF-DCB-2, and (g) CTF-DCB-3 coated columns. The chromatograms of styrene/phenylacetylene mixtures in (d) CTF-DCB-1, (f) CTF-DCB-2, and (h) CTF-DCB-3 coated columns.

equilibrium of the kinetic diffusion and thermodynamic interactions, achieving effective separation of benzene isomers as well as styrene/phenylacetylene mixtures. Thus, modulating the crystallinity is essential for achieving optimal separation performance in porous materials.

Declaration of competing interest

The authors declare that they have no known competing financial interests or personal relationships that could have appeared to influence the work reported in this paper.

CRediT authorship contribution statement

Chu Zeng: Writing – original draft, Investigation, Formal analysis, Data curation. **Han Yang:** Writing – review & editing, Formal analysis. **Ming Xu:** Writing – review & editing, Funding acquisition, Conceptualization. **Zhi-Yuan Gu:** Writing – review & editing, Funding acquisition, Conceptualization.

Acknowledgments

This work was supported by the National Natural Science Foundation of China (Nos. 22174067, 22204078, and 22374077), the Natural Science Foundation of Jiangsu Province of China (No. BK20220370), Jiangsu Provincial Department of Education (No. 22KJB150009), State Key Laboratory of Analytical Chemistry for Life Science (No. SKLACLS2218), the Priority Academic Program Development of Jiangsu Higher Education Institutions, Jiangsu Association for Science and Technology (No. TJ-2023–076), and Shanghai Synchrotron Radiation Facility Beamline BL17B1 (No. 2021-NFPS-PT-006657). We acknowledge Yuxi Xu from Westlake University for the synthesis of the CTF-DCBs.

Supplementary materials

Supplementary material associated with this article can be found, in the online version, at doi:10.1016/j.cclet.2024.110064.

References

[1] Z.R. Tao, J.X. Wu, Y.J. Zhao, et al., Nat. Commun. 10 (2019) 2911.
[2] T. Si, X. Lu, H. Zhang, et al., Chin. Chem. Lett. 33 (2022) 3869–3872.
[3] S.Y. Zhang, C.X. Yang, W. Shi, et al., Chem 3 (2017) 281–289.
[4] A. Patel, S. Aslani, S.K. Firooz, D.W. Armstrong, Chromatographia (2023) 1–10.
[5] N. Chang, X.P. Yan, J. Chromatogr. A 1257 (2012) 116–124.
[6] B. Tang, W. Wang, H. Hou, et al., Chin. Chem. Lett. 33 (2022) 898–902.
[7] H.L. Qian, C.X. Yang, X.P. Yan, Nat. Commun. 7 (2016) 12104.
[8] C. Yuan, W. Jia, Z. Yu, et al., J. Am. Chem. Soc. 144 (2022) 891–900.
[9] W.C. Deng, H.L. Qian, C. Yang, et al., ACS Appl. Mater. Interfaces 15 (2023) 54977–54985.
[10] Z. Wang, W.Q. Xiong, Z.F. Huang, et al., Chirality 34 (2022) 462–472.
[11] H.L. Qian, Z.H. Wang, J. Yang, X.P. Yan, Chem. Commun. 58 (2022) 8133–8136.
[12] J.H. Cavka, S. Jakobsen, U. Olsbye, et al., J. Am. Chem. Soc. 130 (2008) 13850–13851.
[13] F. Vermoortele, B. Bueken, G.Le Bars, et al., J. Am. Chem. Soc. 135 (2013) 11465–11468.
[14] Z. Deng, X. Peng, Y.J. Zeng, CrystEngComm 21 (2019) 1772–1779.
[15] A. Schaate, P. Roy, A. Godt, et al., Chem. Eur. J. 17 (2011) 6643–6651.
[16] A.M. Elewa, A.F. EL-Mahdy, A.E. Hassan, et al., J. Mater. Chem. A 10 (2022) 12378–12390.
[17] X. Huang, C. Sun, X. Feng, Sci. China Chem. 63 (2020) 1367–1390.
[18] J. Li, Y. He, Y. Zou, et al., Chin. Chem. Lett. 33 (2022) 3017–3020.
[19] W. Liang, C.J. Coghlan, F. Ragon, et al., Dalton Trans. 45 (2016) 4496–4500.
[20] R. Xu, Q. Ji, P. Zhao, et al., J. Mater. Chem. A 8 (2020) 7870–7879.
[21] P. Ji, T. Drake, A. Murakami, et al., J. Am. Chem. Soc. 140 (2018) 10553–10561.
[22] G. Ye, Y. Gu, W. Zhou, et al., ACS Catal. 10 (2020) 2384–2394.
[23] X. Zhu, T. Ke, J. Zhou, et al., J. Am. Chem. Soc. 145 (2023) 9254–9263.
[24] S.S. Meng, T. Han, Y.H. Gu, et al., Anal. Chem. 94 (2022) 14251–14256.
[25] C.S. Diercks, O.M. Yaghi, Science 355 (2017) eaal1585.
[26] L. Guo, J. Zhang, Q. Huang, et al., Chin. Chem. Lett. 33 (2022) 2856–2866.
[27] W. Zhang, L. Chen, S. Dai, et al., Nature 604 (2022) 72–79.
[28] L. Ascherl, T. Sick, J.T. Margraf, et al., Nat. Chem. 8 (2016) 310–316.
[29] T. Sun, Y. Liang, Y. Xu, Angew. Chem. Int. Ed. 61 (2022) e202113926.
[30] T. Sun, Y. Liang, W. Luo, et al., Angew. Chem. Int. Ed. 61 (2022) e202203327.
[31] L. Ettre, J. High. Resolut. Chromatogr. 10 (1987) 221–230.
[32] L.M. Blumberg, J. Chromatogr. A 1524 (2017) 303–306.
[33] J. Nikelly, Anal. Chem. 44 (1972) 623–625.
[34] Z.Y. Gu, X.P. Yan, Angew. Chem. 122 (2010) 1519–1522.